

Identification of the Molecular Mechanisms by Which the Diterpenoid Salvinorin A Binds to κ -Opioid Receptors[†]

Feng Yan,^{‡,§} Philip D. Mosier,^{‡,||} Richard B. Westkaemper,^{||} Jeremy Stewart,[⊥] Jordan K. Zjawiony,[⊥] Timothy A. Vortherms,[§] Douglas J. Sheffler,[§] and Bryan L. Roth^{*,§,¶}

Departments of Biochemistry, Psychiatry, and Neurosciences and Comprehensive Cancer Center, Case Western Reserve University Medical School, Cleveland, Ohio 44106, Department of Medicinal Chemistry, Virginia Commonwealth University, Richmond, Virginia 23284, and Department of Pharmacognosy, University of Mississippi, University, Mississippi 38677

Received March 16, 2005; Revised Manuscript Received May 2, 2005

ABSTRACT: Salvinorin A is a naturally occurring hallucinogenic diterpenoid from the plant *Salvia divinorum* that selectively and potently activates κ -opioid receptors (KORs). Salvinorin A is unique in that it is the only known lipid-like molecule that selectively and potently activates a G-protein coupled receptor (GPCR), which has as its endogenous agonist a peptide; salvinorin A is also the only known non-nitrogenous opioid receptor agonist. In this paper, we identify key residues in KORs responsible for the high binding affinity and agonist efficacy of salvinorin A. Surprisingly, we discovered that salvinorin A was stabilized in the binding pocket by interactions with tyrosine residues in helix 7 (Tyr313 and Tyr320) and helix 2 (Tyr119). Intriguingly, activation of KORs by salvinorin A required interactions with the helix 7 tyrosines Tyr312, Tyr313, and Tyr320 and with Tyr139 in helix 3. In contrast, the prototypical nitrogenous KOR agonist U69593 and the endogenous peptidergic agonist dynorphin A (1–13) showed differential requirements for these three residues for binding and activation. We also employed a novel approach, whereby we examined the effects of cysteine-substitution mutagenesis on the binding of salvinorin A and an analogue with a free sulfhydryl group, 2-thiosalvinorin B. We discovered that residues predicted to be in close proximity, especially Tyr313, to the free thiol of 2-thiosalvinorin B when mutated to Cys showed enhanced affinity for 2-thiosalvinorin B. When these findings are taken together, they imply that the diterpenoid salvinorin A utilizes unique residues within a commonly shared binding pocket to selectively activate KORs.

Salvinorin A (Figure 4) is the major active ingredient of *Salvia divinorum*, a hallucinogenic plant that has been used historically in the traditional shamanic practices of the Mazatec people of Oaxaca, Mexico (1–3). We recently discovered that salvinorin A, a neutral diterpenoid, activates κ -opioid receptors (KORs)¹ (4) and is unique in that it represents the only known lipid-like small molecule that selectively and potently activates a peptidergic G-protein coupled receptor (GPCR) (5, 6). Salvinorin A is highly selective for KOR and has no significant activity at μ , δ , or ORL1-opioid receptors (4, 7) nor other tested GPCRs, neurotransmitter transporters, or ion channels (4). Because of its unique structure and selectivity for a single GPCR,

[†] This research was supported in part by RO1DA017204, KO2MH01366, and the NIMH Psychoactive Drug Screening Program to B.L.R.

* To whom correspondence should be addressed: Department of Biochemistry, RM W441, School of Medicine, Case Western Reserve University, 2109 Adelbert Road, Cleveland, OH 44106. Telephone: 216-368-2730. Fax: 216-368-3419. E-mail: bryan.roth@case.edu.

[‡] These authors contributed equally to this work.

[§] Department of Biochemistry, Case Western Reserve University Medical School.

^{||} Virginia Commonwealth University.

[⊥] University of Mississippi.

[¶] Departments of Psychiatry and Neurosciences and Comprehensive Cancer Center, Case Western Reserve University Medical School.

¹ Abbreviations: KOR, κ -opioid receptor; GPCR, G-protein coupled receptor.

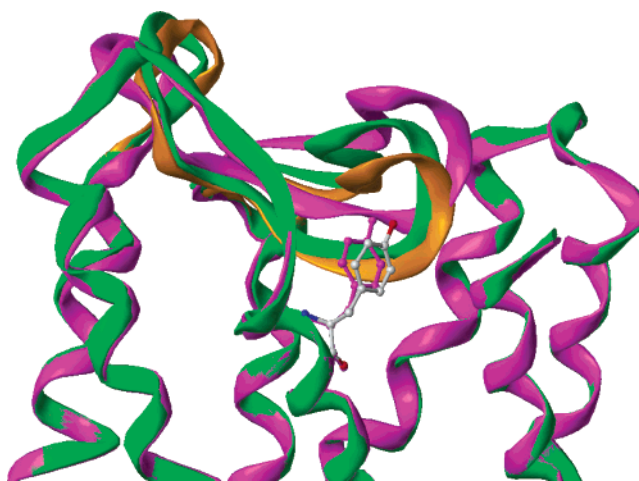


FIGURE 1: Comparison of the e2 loop structures. Comparison of the e2 loop structures from the initial minimized KOR (orange), the MD-averaged and minimized structure (green), and the minimized structure of the MD snapshot taken at 2225 fs (magenta). The position of Tyr313 in TM7 is illustrated.

the salvinorin A-KOR receptor–ligand complex provides a model system for exploring the molecular and atomic features responsible for small-molecule selectivity among highly homologous receptors. Salvinorin A also provides a tool for further study of the activation mechanisms of GPCRs.

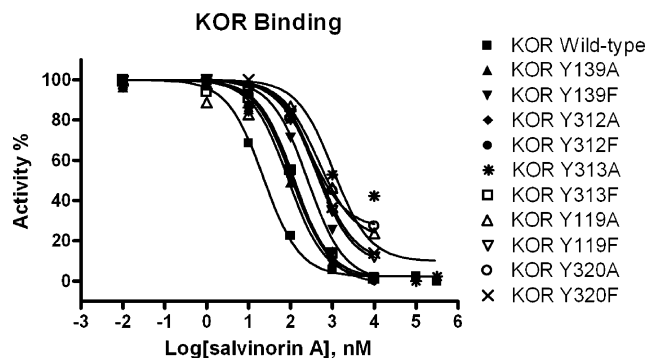


FIGURE 2: Effects of various mutations on salvinorin A binding to KORs reveals the importance of Y313. Shown are representative competition binding isotherms for inhibition of 3H-diprenorphine binding to cloned KORs transiently expressed in HEK-293-T cells. Curves represent the theoretical fits for a single binding site model. K_i values are found in Table 2. For the sake of clarity, error bars are omitted but were typically $<10\%$.

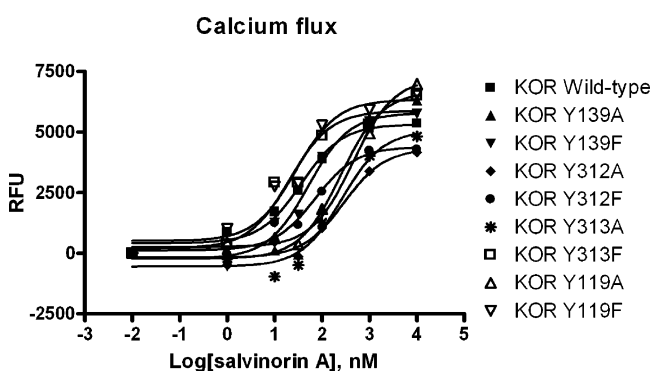


FIGURE 3: Activation of wt and mutant KORs by salvinorin A. Shown are representative dose-response studies for activation of wt and mutant KORs transiently expressed in HEK-293 cells (see the Experimental Procedures for assay details). Curves represent the theoretical fits for the parameter estimates provided in Table 3; for purposes of clarity, error bars are omitted but were typically $<10\%$.

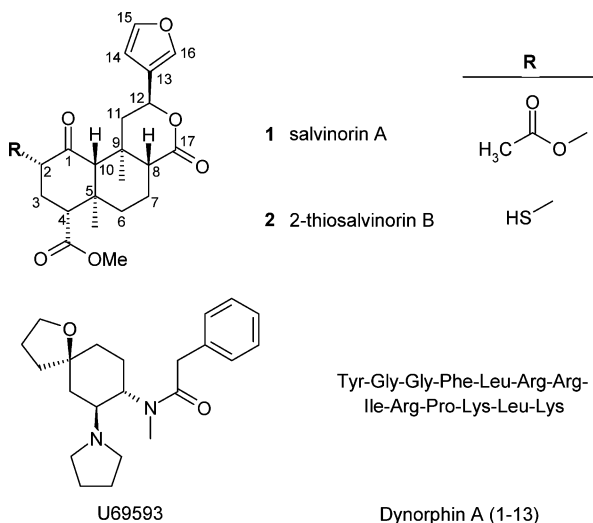


FIGURE 4: Structures of salvinorin A and other compounds used in the current studies.

The binding pocket of the KOR will not be known with certainty until the structure of a KOR-ligand complex is solved. In the absence of direct structural information, combined molecular modeling/mutagenesis studies can provide testable models for ligand interactions and activation

mechanisms (8–10), and we and others have used these approaches with great success for biogenic amine (9, 11) and peptide (4, 12) receptors. Historically, attention has been focused on ionic interactions and hydrogen-bond-type interactions between ligands (either small molecule or peptidic) and highly conserved charged residues (e.g., Asp and Glu) or residues capable of forming hydrogen bonds (e.g., Tyr and Arg) for anchoring and orienting ligands in the binding pocket (see ref 8 for a review). Because salvinorin A possesses no ionizable groups, ionic interactions cannot provide stability in the binding pocket, although it is conceivable that hydrogen-bond-type interactions could be involved (4).

In the current study, we examined the molecular and atomic features essential for the binding and activation of KORs by salvinorin A. Previous computer modeling predicted the key residues that are believed to contribute in salvinorin A binding to KOR: Tyr313, Gln115, Tyr312, and Tyr139 (4). To determine if these residues are involved in salvinorin A binding, KOR mutants were constructed and the binding site between salvinorin A and KOR was investigated via radioligand binding and functional and molecular modeling studies. We also employed a novel combined chemical-mutagenesis approach, whereby the effects of cysteine-substitution mutageneses were evaluated for a novel salvinorin A analogue that possesses a free sulfhydryl group.

EXPERIMENTAL PROCEDURES

Materials. Standard reagents, unless stated otherwise, were purchased from Sigma-Aldrich (St. Louis, MO). [^3H]-Diprenorphine ($K_d = 0.2$ nM to KOR; 50 Ci/mmol) was obtained from PerkinElmer-LifeScience Inc. The XL2-Blue *Escherichia coli* strain was purchased from Stratagene (La Jolla, CA). Two sources of salvinorin A were used for the studies described here: Biosearch and the *Salvia divinorum* Research and Information Center, Malibu, CA.

The human KOR cDNA was obtained from the Guthrie Research Foundation (GenBank accession number NM000912) and subcloned into the eukaryotic expression vector pIRESneo (Invitrogen, Carlsbad, CA). $G_{\alpha 16}$ was obtained from the Guthrie Research Foundation; both constructs were verified by automated dsDNA sequencing (Cleveland Genomics, Inc., Cleveland, OH) before use. A stable line expressing the human KOR (hKOR-293) was obtained by transfecting a hKOR expression vector (hKOR-pIRESneo) into human embryonic kidney-293 cells and selecting in 600 $\mu\text{g}/\text{mL}$ G418. The cells were maintained and transfected as previously detailed (4). Surviving clones were expanded and characterized with one (hKOR-293) that expressed high levels of hKOR (ca. 1 pmol/mg) used for further studies.

2-Thiosalvinorin B Synthesis. Salvinorinyl chloride (16 mg, 40 μmol) was placed in DMF (2 mL) containing sodium hydrogen sulfide (6.4 mg, 114 μmol), and the mixture was heated to 35–40 $^{\circ}\text{C}$ for 1 h. Brine water (2 mL) was added, and the mixture was extracted 3 times with ethyl acetate (5 mL). The combined organic extracts were concentrated in vacuo, and the residue was redissolved in acetone (HPLC grade, 1 mL) and separated by HPLC (C_{18} column, MeCN/ H_2O 1:1, detection at 210 nm). 2-Thiosalvinorin B (6.9 mg, 44% yield) was collected at $R_t = 8.9$ min. Complete details

of synthesis and chemical characterization will be reported separately (13) (Stewart et al., manuscript in preparation)

Site-Directed Mutagenesis. The mutations were introduced using the Quickchange mutagenesis kit from Stratagene according to the recommendations of the manufacturer. The presence of the mutations was verified by automated dsDNA sequencing (Cleveland Genomics, Inc., Cleveland, OH) before use. Clones expressing high and comparable levels of KOR mutants were studied by radioligand saturation and competition binding experiments as described later.

Radioligand Binding Assays. Radioligand binding assays were performed as previously detailed (4). In brief, crude cell membranes were prepared by lysing transfected HEK-T cells in binding buffer (50 mM Tris-Cl, 10 mM MgCl₂, and 0.1 mM EDTA at pH 7.40) and centrifugation at 30000g for 20 min. Membrane pellets were then stored at -80 °C until use in binding assays. Binding assays were conducted in total volumes of 0.2 mL in 96-well plates in a binding buffer containing 0.1–0.2 nM ³H-diprenorphine with 10 μM naloxone to determine nonspecific binding for a total of 60 min at room temperature. Assays were terminated by harvesting over GF-C Whatman filters, which had been pre-equilibrated with 0.01% polyethyleneimine and 3 quick washes with ice-cold binding buffer. After the filters had dried, they were counted by liquid scintillation spectrometry. *K_i* determinations were performed by using six concentrations of unlabeled ligand spanning a 10 000-fold dose range. The raw data was analyzed by Prism 4.01 (GraphPad Software, Inc., San Diego, CA) to give *K_i* values reported as the mean ± standard error of the mean (SEM).

Functional Assays. Functional assays using wild-type and mutant KORs were performed as previously detailed (14). Briefly, wild-type and mutant receptors were cotransfected with Gα₁₆ into HEK-293 cells, and measurements of agonist-induced intracellular Ca²⁺ release were monitored using a Molecular Devices FLEXSTATION II (see ref 15 for details). The raw data were analyzed by Prism 4.01 (GraphPad Software, Inc., San Diego, CA) to give EC₅₀ and *E*_{max} values.

κ-Opioid Receptor Modeling and Ligand Docking. Modeling studies were performed using SYBYL (version 6.9.2, 2004, Tripos Associates, Inc., St. Louis, MO), and a new KOR model was constructed using a rhodopsin template essentially as previously described for the 5-HT_{2A} receptor (15). An unambiguous alignment of the rhodopsin and KOR sequences was performed manually by matching the highly conserved residues in transmembrane helices previously identified (16, 17). Because the sequences of the KOR and rhodopsin are similar in length, there are very few insertions (four) and deletions (two) evident in the alignments of the KOR and rhodopsin sequences in the structurally important extra- and intracellular loops; the helical segments contained no insertions or deletions. The COMPOSER module of SYBYL was used to construct an initial model from an experimental bovine rhodopsin structure (A chain of 1F88) (17). Amino acid side-chain geometries for the KOR receptor model were established from backbone-dependent libraries of rotamer preference using SCWRL (18). The helix backbone geometry of rhodopsin was transferred without change in this procedure. The PROBABLE facility within SYBYL was used to identify sites of unusual and sterically clashing side-chain geometries that were interactively cor-

rected as necessary. Model minimizations were performed using the Tripos Force Field using Gasteiger–Huckel charges with a distance-dependent dielectric constant = 4 and nonbonded cutoff = 8 Å to a gradient of 0.05 kcal/(mol Å).

The KOR model was further modified by minimization with an ensemble of known agonists (bremazocine, morphine, MPCB, U69593, and 6'-GNTI) docked into the receptor. The ensemble of structurally diverse κ agonists was created by successive superimposition of ligands according to previous suggestions based on known structure activity relationships in addition to obvious structural similarities (19, 20). A model of a complex between the antagonist nor-BNI and KOR served as the starting point for subsequent superimpositions. This initial complex was generated by interactive docking of nor-BNI in a fashion consistent with probable interactions with H291, D138, and E297 of the KOR (21–23).

To explore the inherent flexibility of the e2 loop and the effects of the e2 loop in limiting ligand access to Tyr313, molecular dynamics (MD) simulations were performed. The N terminus of the rhodopsin structure folds over the β turn of the e2 loop. It has been previously shown that the N-terminal region is not necessary for binding to the MOR (24, 25). In addition, there was little similarity in sequence or length between the N termini of rhodopsin and the KOR. Thus, in preparation for the MD simulations, the N terminus of the KOR was removed so as not to constrain the e2 loop during the simulation. The residues deleted included all those up to but not including Pro56. The orientation of the Tyr313 side chain in the original KOR model was directed away from the interior of the receptor ($\chi_1 = 67.8^\circ$). To explore the possibility of direct ligand interaction with Tyr313, its side-chain position was adjusted so that it would be accessible from the interior of the KOR ($\chi_1 = 275.0^\circ$). In its new position, Tyr313 is projected toward and can potentially interact with residues in the e2 loop, including Val205, Asp206, Ile208, and Glu209. An MD simulation was performed for 100 ps using the default settings of the MD routine within SYBYL and maintaining all residues except the e2 loop (Val195–Asp223) as an aggregate to observe the behavior of the loop. The position of the backbone of residues Cys210, Ser211, and Leu212 during the MD run remained close to the interior cavity of the receptor, and their positions in the averaged structure are relatively close to the corresponding backbone atoms in the original KOR. At no time during the simulation did the e2 loop completely exit the interior cavity of the KOR. An average KOR structure was then generated from individual MD conformations and was subsequently energy-minimized. In addition, a snapshot from the MD run at 2225 fs when the loop was farthest from the binding pocket and Glu209 was hydrogen-bonded to Tyr313 was selected and minimized, providing a KOR model with a greater accessibility to Y313 (Figure 1).

GOLD version 2.2 (26, 27) was used to dock salvinorin A and 2-thiosalvinorin B into the MD-averaged and minimized KOR model and into the minimized MD snapshot model. Prior to docking, the CONCORD routine within SYBYL was used to assign initial conformations to salvinorin A and 2-thiosalvinorin B. Several GOLD studies were performed, representing three distinct GOLD configurations. In the first GOLD configuration, standard default settings (no speed-up) for the genetic algorithm (GA) and annealing

Table 1: Residues within Specified Heavy-Atom Distances between the Salvinorin A Ligand and the KOR Receptor for the Proposed Binding Mode^a

| 3.0 Å | 3.5 Å | 4.0 Å | 4.5 Å | 5.0 Å |
|-------|-------|-------|-------|-------|
| none | I135 | Y66 | M112 | Y139 |
| | D138 | Y119 | A298 | P215 |
| | E209 | V134 | | |
| | C210 | S211 | | |
| | I294 | L212 | | |
| | Y313 | F214 | | |
| | I316 | E297 | | |
| | Y320 | Y312 | | |

^a Receptor atoms may be part of the backbone or the side chain.

parameters were used and 10 individual GA runs were performed. A large active-site radius of 25.0 Å about the Asp138 γ -carbon atom was used to define the receptor site, thus allowing for the possibility of direct interaction of salvinorin A with distant residues, including Tyr313. In the second GOLD configuration, the GA and annealing parameters corresponding to the 3 \times speedup option in GOLD were used and 30 individual GA runs were performed. A somewhat more focused 15-Å radius about the Tyr313 side-chain oxygen atom was used to define the receptor site. A third configuration, used only with the minimized MD snapshot at 2225 fs, was identical to the second configuration with the exception that a 20.0-Å radius was used. In each GOLD configuration, cavity detection and ring corner flipping were enabled and the GoldScore scoring function was used to rank the docked solutions. Final docked complexes were evaluated interactively, and ligand rotatable bonds and amino acid residue side-chain torsion angles were scanned manually to estimate the probability that dipolar ligand-side-chain interactions could occur in a stereoelectronically favorable fashion. The complexes were then energy-minimized to identify and resolve any remaining strain within the system. From among all top-ranked docked solutions, one distinct family of docked complexes was selected to represent the dominant binding mode based on its ability to account for all of the observed mutation effects described in this work. The final model was selected from a study representing the third GOLD configuration.

All molecular modeling was carried out on IRIX 6.5-based Silicon Graphics, Inc. workstations.

RESULTS

Radioligand Binding and Functional Parameters of Native and Mutant KORs Reveal Differential Modes of Agonist Binding and Activation. We performed site-directed mutagenesis studies and characterized the binding and functional parameters of the mutated KORs. All of the mutants were expressed at high levels in HEK 293T cells and all had comparable affinity for the antagonist [³H]-diprenorphine (Table 2) and natural agonist dynorphin A (1–13), with the exceptions of the Y139F (8-fold attenuation), Y119F and Y320F (6-fold attenuation each), and Y119A (4-fold attenuation). These results demonstrate that the mutations studied did not significantly alter KOR receptor expression nor significantly perturb the topology of the receptor because binding for the high-affinity antagonist and endogenous agonist dynorphin were not greatly attenuated (e.g., <10-fold change in affinities).

In 4 of 10 of the studied KOR mutants, the affinity for salvinorin A was not significantly altered from wild-type KOR (Table 2). However, a dramatic decrease in the affinity of salvinorin A was obtained by introducing a single mutation, Y313A on TM7 ($K_i = 694$ nM, 22-fold decrease), a smaller effect was seen for U69369 binding, and no significant effect was seen for dynorphin A (1–13). These results were predicted by our previously published modeling studies (4). To elucidate the molecular mechanism(s) responsible for the selective interaction of salvinorin A with Tyr313, we examined a Y313F mutation that should maintain hydrophobic interactions and should abolish hydrogen-bond-type interactions between the –OH of Tyr313 and salvinorin A. Surprisingly, the Y313F mutation caused no loss of the binding affinity, indicating that hydrophobic interactions between salvinorin A and Tyr313 provide stabilization of salvinorin A in the binding pocket.

Of the other tested mutations, the mutations at the Tyr119 and Tyr320 loci had significant effects, while mutations at the Tyr139 locus had modest effects (<10-fold change) on the affinity of salvinorin A for KOR. It appears that the primary mode of interaction at Tyr119 and Tyr320 is via hydrogen bonding: in each case, the majority of the affinity was lost on the mutation from Tyr to Phe; little additional perturbation resulted from the Tyr to Ala mutation. The affinities of U69593 and dynorphin A (1–13) were, in

Table 2: Affinity (K_i , nM) of Salvinorin A, U69593, and Dynorphin A (1–13) Binding to the Wild-Type KOR and Mutants Transiently Expressed in HEK 293 T Cells

| KOR | K_d (nM) ^a | B_{max} (pmol/mg) ^a | salvinorin A | | U69593 | | dynorphin A (1–13) | |
|-----------|-------------------------|----------------------------------|-------------------------|--------------------|-------------------------|--------------------|-------------------------|--------------------|
| | | | K_i (nM) ^b | ratio ^c | K_i (nM) ^b | ratio ^c | K_i (nM) ^b | ratio ^c |
| wild type | 0.25 ± 0.02 | 5.8 ± 2.0 | 31.6 ± 6.5 | | 11.7 ± 3.4 | | 1.75 ± 0.35 | |
| Y139A | 0.26 ± 0.07 | 8.3 ± 2.5 | 53.9 ± 13.9 | 2 | 20.6 ± 4.0 | 2 | 1.98 ± 0.41 | 1 |
| Y139F | 0.59 ± 0.28 | 5.0 ± 1.0 | 193 ± 38 | 6 | 101 ± 29 | 9 | 13.3 ± 4.6 | 8 |
| Y312A | 0.55 ± 0.10 | 2.7 ± 0.4 | 88.6 ± 10.9 | 3 | 52.6 ± 11.3 | 4 | 1.79 ± 0.28 | 1 |
| Y312F | 0.18 ± 0.03 | 4.4 ± 0.6 | 65.1 ± 11.0 | 2 | 53.0 ± 12.5 | 5 | 1.39 ± 0.22 | 1 |
| Y313A | 0.72 ± 0.18 | 14.9 ± 0.8 | 694 ± 106 | 22 | 107 ± 32 | 9 | 4.10 ± 0.78 | 2 |
| Y313F | 0.26 ± 0.03 | 7.0 ± 0.1 | 63.3 ± 15.2 | 2 | 37.0 ± 5.0 | 3 | 0.93 ± 0.14 | 1 |
| Y119A | 0.19 ± 0.004 | 1.41 ± 0.02 | 342 ± 40 | 11 | 59.9 ± 2.4 | 5 | 6.71 ± 0.89 | 4 |
| Y119F | 0.32 ± 0.09 | 3.6 ± 0.2 | 233 ± 66 | 7 | 90.7 ± 5.3 | 8 | 11.3 ± 4.8 | 6 |
| Y320A | 0.92 ± 0.004 | 1.3 ± 0.1 | 380 ± 103 | 12 | 195 ± 34 | 17 | 3.15 ± 0.82 | 2 |
| Y320F | 0.82 ± 0.33 | 1.7 ± 0.6 | 301 ± 75 | 10 | 276 ± 88 | 24 | 9.68 ± 2.84 | 6 |

^a Saturation binding of ³H-diprenorphine to the wild type and mutants was performed. Data represent, in mean ± SEM form, two or three independent experiments. ^b The affinity constants (K_i) of the different compounds were determined in competition binding assays with ³H-diprenorphine and increasing concentrations of unlabeled compounds. Each value is the mean of three or four independent experiments (see the Experimental Procedures for details). ^c For each compound, the ratio is $K_{i(\text{mutant})}/K_{i(\text{wild-type})}$.

Table 3: Agonist Potency (EC_{50} , nM)^a and Relative Agonist Efficacy (Normalized E_{max})^a of Salvinorin A, U69593, and Dynorphin A (1–13) for the Wild-Type KOR and Mutants Transiently Expressed in HEK 293 Cells

| KOR | salvinorin A | | | U69593 | | | dynorphin A (1–13) | | |
|-----------|-----------------|--------------------|-----------------|----------------|--------------------|--------------------|--------------------|--------------------|--------------------|
| | EC_{50} (nM) | ratio ^b | E_{max} (RFU) | EC_{50} (nM) | ratio ^b | relative E_{max} | EC_{50} (nM) | ratio ^b | relative E_{max} |
| wild type | 45.8 ± 8.1 | | 3232 ± 728 | 23.6 ± 6.4 | | 1.13 ± 0.19 | 343 ± 54 | | 1.53 ± 0.26 |
| Y139A | 240 ± 44 | 5 | 4893 ± 795 | 140 ± 38 | 6 | 1.13 ± 0.29 | 1044 ± 258 | 3 | 1.07 ± 0.15 |
| Y139F | 47.0 ± 22.2 | 1 | 5265 ± 952 | 13.3 ± 3.6 | 1 | 1.00 ± 0.15 | 369 ± 98 | 1 | 1.17 ± 0.18 |
| Y312A | 189 ± 46 | 4 | 4667 ± 589 | 451 ± 225 | 19 | 0.93 ± 0.12 | 416 ± 86 | 1 | 0.87 ± 0.18 |
| Y312F | 68.3 ± 22.1 | 1 | 4308 ± 526 | 98.0 ± 33.4 | 4 | 1.03 ± 0.09 | 172 ± 39 | 1 | 1.30 ± 0.12 |
| Y313A | 275 ± 53 | 6 | 5124 ± 705 | 43.9 ± 3.3 | 2 | 1.17 ± 0.12 | 233 ± 44 | 1 | 1.23 ± 0.19 |
| Y313F | 49.6 ± 15.6 | 1 | 5127 ± 747 | 48.9 ± 12.1 | 2 | 0.97 ± 0.42 | 91 ± 3.4 | 0.3 | 1.17 ± 0.52 |
| Y119A | 434 ± 163 | 9 | 5004 ± 718 | 358 ± 181 | 15 | 0.80 ± 0.26 | 1290 ± 634 | 4 | 0.80 ± 0.26 |
| Y119F | 43.5 ± 14.7 | 1 | 3880 ± 770 | 35.9 ± 13.5 | 2 | 0.80 ± 0.15 | 276 ± 99 | 1 | 1.03 ± 0.03 |
| Y320A | ND ^c | | ND | ND | | ND | ND | | ND |
| Y320F | ND | | ND | ND | | ND | ND | | ND |

^a EC_{50} and relative E_{max} were determined from calcium flux assays as described under the Experimental Procedures. The results represent the average of three independent experiments with normalized E_{max} values in mean ± SEM form. ^b For each compound, the ratio is $EC_{50}(\text{mutant})/EC_{50}(\text{wild-type})$. ^c ND = no detectable agonist activity; mutants Y320A and Y320F have no response to salvinorin A, U69593, or dynorphin A (1–13).

general, only modestly affected by the various mutations, with the possible exception of Y320A and Y320F. Interestingly, the single mutation, which had the greatest effect on the affinity of salvinorin A (Y313A) attenuated the affinity of U69593 9-fold and had an insignificant effect on dynorphin A (1–13) affinity (Table 2).

We next determined the agonist potencies and efficacies of salvinorin A, U69593, and dynorphin A (1–13) at wild-type and mutant KORs (Table 3). As expected, the Y313A mutation significantly attenuated the potency of salvinorin A (6-fold), while the Y119A mutation decreased agonist potency 9-fold. Surprisingly, several other mutations attenuated the potency of salvinorin A for activating KORs: Y139A (5-fold) and Y312A (4-fold). These results were intriguing because Y139A and Y312A did not affect binding of salvinorin A to the KOR. The most severe effect was found by mutations Y320A and Y320F. They abolished agonist-induced activation of KOR by all three tested compounds: salvinorin A, U69593, and dynorphin A (1–13). Aside from the Y320 mutations, Y139A (3-fold) and Y119A (4-fold), dynorphin A (1–13) tolerated mutations without losing agonist efficacy. U69593 showed a dramatic loss of potency for activation for the Y312A (19-fold) and Y119A (15-fold) mutations. As with the other compounds, the agonist potency of U69593 was diminished by Y139A 6-fold. In contrast to salvinorin A (6-fold), Y313A only has a 2-fold effect on the ability of U69593 to activate KOR.

Molecular Modeling Predictions. A family of docked solutions was generated for salvinorin A using automated docking techniques (see the Experimental Procedures for details); this family is represented by the model shown in parts A–C of Figure 5. The closest sites of interaction are between salvinorin A and TM1–3, TM6, TM7, and the extracellular loop e2 of the receptor model. In our model, the 2-acetoxy group of salvinorin A is positioned between the e2 loop and the top of TM7 near Tyr313 and the furan ring hydrogen-bonds with Tyr320 in TM7 and Tyr119 in TM2. The 4-methyl ester group is oriented toward the top of TM6. Other models representing different families of docked solutions were also obtained, although they did not account for as many of the observed mutational effects (not shown).

All of the mutated residues in the current model point approximately toward the central cavity, with the exceptions

of Leu309 and Ser210, while Tyr312 and Tyr313 are located more remotely near the top of the binding cavity. Table 1 lists the distances between heavy atoms of salvinorin A and nearby amino acid residues in the KOR. Mutations of some of the residues within a distance of 4 Å have been shown by others to affect the binding of conventional KOR ligands. These include Asp138, the putative ammonium-binding residue (28); Cys210, the e2 loop disulfide-forming cysteine (29); and Ile294, which has been implicated in a SCAM study (30). While present in the binding cavity, Tyr139 was not predicted to interact significantly with the docked ligand.

Cys Substitutions Enhance the Binding of 2-Thiosalvinorin B. To more fully elucidate the binding mode of salvinorin A, we examined the binding of a newly synthesized salvinorin A analogue, 2-thiosalvinorin B (**2**) at the wild type and Cys-substituted KOR mutants. We reasoned that Cys substitutions should show enhanced affinity for 2-thiosalvinorin B if the Cys residue was in close proximity to the –SH moiety of 2-thiosalvinorin B. Because the KOR has a single Cys in the binding pocket (Cys315; 30), we initially characterized C315S. As shown in Table 4, the C315S did not significantly alter the binding of either salvinorin A or 2-thiosalvinorin B. On the basis of the salvinorin A binding model, we constructed several cysteine substitutions in the background of C315S, including Y119C, I294C, E297C, L309C, S310C, and Y313C (Table 4) of which Ile294, Glu297, Leu309, Ser310, and Tyr313 are unique to KORs. As predicted by the salvinorin A binding model, the Y313C mutation *preserved* the affinity of 2-thiosalvinorin B because the –SH group is predicted to be in close proximity to the Cys substitution at the 313 locus in the C315S background. In contrast, the affinity of salvinorin A for the Y313C–C315S double mutant *decreased* by 14.2-fold, presumably because the 2-acetoxy group of salvinorin A cannot form interactions with C313 as effectively or as strongly as 2-thiosalvinorin B. Additionally, I294 and E297, when mutated to Cys, gave rise to significantly enhanced affinities for *both* salvinorin A and 2-thiosalvinorin B.

DISCUSSION

The major finding of this paper is the discovery that a diterpenoid (salvinorin A) utilizes a novel mode for peptidergic GPCR (KOR) binding and activation. We also provide new molecular models that provide reasonable atomic-level

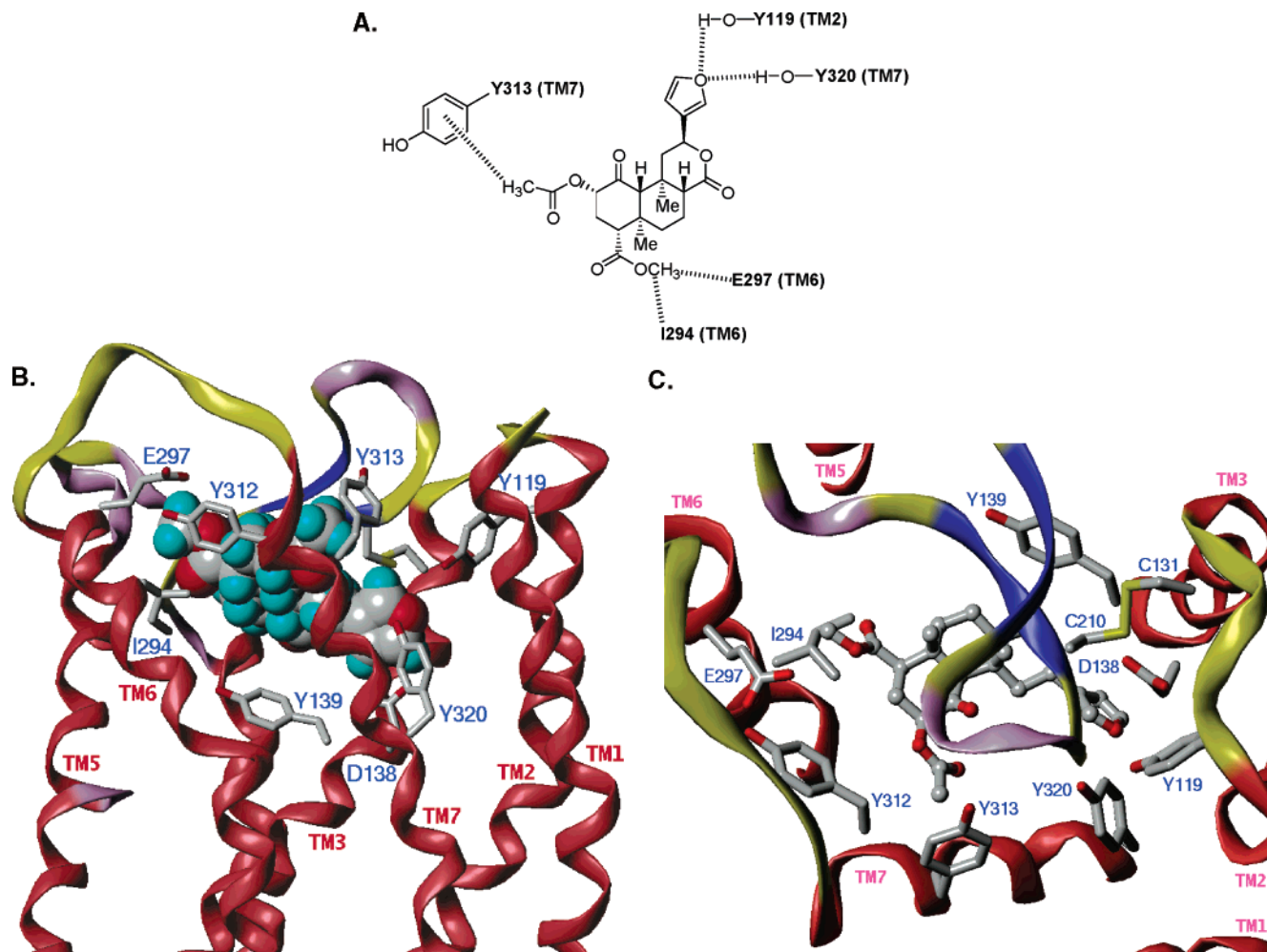


FIGURE 5: Modeling salvinorin A-KOR interactions. (A) Two-dimensional representation of the proposed interactions between salvinorin A and various side chains in the KOR-binding site. (B) Proposed binding mode of salvinorin A in the KOR, looking through the extracellular side of the helical bundle. Tyr313 and Tyr320 in TM7 are nearest to the viewer. The KOR is color-coded based on the assignment of the secondary structure using the Kabsch-Sander (34) algorithm (red = helix, blue = β sheet, violet = turn, and yellow = coil). The ligand is rendered as a CPK-style space-filling model. (C) View of the proposed binding model of salvinorin A looking from the extracellular side of the KOR beyond the e2 loop to the binding pocket. For clarity, the intracellular portion of the KOR is not displayed. The ligand is rendered as a ball-and-stick figure, and important nearby residues are rendered as capped stick figures.

Table 4: Effect of Cys-Substitution Mutations^a on Salvinorin A and 2-Thiosalvinorin B Binding to KORs

| KOR | salvinorin A | | 2-thiosalvinorin B | | | U69593 | |
|-------------|-------------------------|--------------------|-------------------------|--------------------|--------------------|-------------------------|--------------------|
| | K_i (nM) ^b | ratio ^c | K_i (nM) ^b | ratio ^c | ratio ^d | K_i (nM) ^b | ratio ^c |
| wild type | 39.6 ± 14.5 | | 157 ± 40 | | 4.0 | 15.4 ± 3.2 | |
| C315S | 37.6 ± 17.6 | | 202 ± 72 | | 5.4 | 54.3 ± 8.2 | |
| C315S-Y313C | 536 ± 66 | 14.2 | 219 ± 57 | 1.1 | 0.4 | 59.6 ± 6.5 | 1.1 |
| C315S-Y119C | 178 ± 54 | 4.7 | 226 ± 49 | 1.1 | 1.3 | 220 ± 83 | 4.1 |
| C315S-I294C | 6.64 ± 2.71 | 0.2 | 43.3 ± 3.8 | 0.2 | 6.5 | 8.26 ± 1.78 | 0.2 |
| C315S-E297C | 4.21 ± 0.89 | 0.1 | 36.3 ± 2.1 | 0.2 | 8.6 | 4.88 ± 1.89 | 0.1 |
| C315S-L309C | 20.3 ± 8.9 | 0.5 | 92.7 ± 38.8 | 0.5 | 4.6 | 194 ± 97 | 3.6 |
| C315S-S310C | 34.9 ± 8.9 | 0.9 | 347 ± 83 | 1.7 | 10.0 | 78.2 ± 21.1 | 1.4 |
| C315S-Y320C | NA | | NA | | | NA | |
| C315S-Y66C | 66.9 ± 21.2 | 1.8 | 214 ± 30 | 1.1 | 3.2 | 180 ± 42 | 3.3 |

^a The double mutants were based on C315 (7.38), which is conserved among the opioid receptor family and is differentially accessible [Xu, et al. (2000) *Biochemistry* 39, 13904–13915]. ^b The affinity constants (K_i) of the different compounds were determined in competition binding assays with ³H-diprenorphine and increasing concentrations of unlabeled compounds. Each value is the mean of two or three independent experiments (see the Experimental Procedures for details). ^c For each compound, the ratio is $K_{i(\text{mutant})}/K_{i(\text{C315S})}$. ^d For each compound, the ratio is $K_{i(2\text{-thiosalvinorin B})}/K_{i(\text{salvinorin A})}$.

explanations for the highly selective binding of a diterpenoid, salvinorin A, to a peptide receptor, the KOR. We also report a novel approach, whereby a designed cysteine-substitution mutagenesis is shown to differentially affect the affinity of salvinorin A and of a salvinorin A derivative with a free

sulfhydryl moiety. These results are important because they demonstrate that the exquisitely potent and efficacious interactions of salvinorin A with KORs are due to novel modes of binding within a common three-dimensional space shared by structurally diverse agonists, each of which utilizes

different residues for binding and activating KORs.

Molecular Modeling Considerations. The e2 loop of rhodopsin and most likely all family A GPCRs are connected to a Cys residue near the extracellular side of TM3 by a disulfide bond. In the proposed salvinorin A–KOR binding model, the ligand is docked near the extracellular opening of the binding pocket. One of the most unanticipated features of the rhodopsin structure is that the β hairpin of the e2 loop lies deep in within the helix aggregate and actually comprises part of the retinal-binding site. It has been argued that this feature is unlikely to be conserved in aminergic GPCRs because it may limit access of reversibly bound ligands to the binding site (31). However, a recent SCAM investigation of the e2 loop of the dopamine D2 receptor suggests that its structure is rhodopsin-like (10). In addition, it has been shown that His319 of TM7 and Asp216 of the e2 loop of the μ -opioid receptor are responsible for the Zn^{2+} -mediated sensitivity of ligand affinity, indicating that these residues are in reasonably close ($C\beta$ – $C\beta$, 6 Å) proximity (32). The distance between the cognate residues, Tyr313 and Glu209, in the rhodopsin-like e2 loop of the KOR models presented here is approximately 8 Å ($C\beta$ – $C\beta$). These observations, coupled with the demonstration of the necessity of a disulfide bond with the e2 loop, (29) imply that the modeled loop structure is accurate.

In the salvinorin A binding model described here, the mutated residues pointed toward a central cavity, although some are clearly less sterically accessible to bound ligands, particularly Tyr312 and Tyr313. Neither Y312A nor Y312F mutations affect the affinity of salvinorin A for the KOR. This is consistent with the proposed model, which indicates only a weak interaction with Tyr312. Interestingly, the Y313A mutation has a large effect on affinity (22-fold), while Y313F has no significant effect. The results of the Y313A and Y313F mutations are consistent with Tyr313 stabilizing the ligand via a hydrophobic-type interaction and with our docked salvinorin A model, which predicts a direct hydrophobic interaction with Tyr313. Although potentially accessible to small molecules, Tyr313 was positioned in a more remote area at the top of the binding cavity interacting with residues in the e2 loop. Tyr313 was previously proposed to provide a hydrogen bond to the 2-acetoxy carbonyl of salvinorin A (4) based on docking studies performed using a *de novo* model developed by Mosberg's group (33). The current model that is based explicitly on the experimental rhodopsin crystal structure shows a substantial difference in the disposition of Tyr313. The fact that Y313F has no effect on ligand affinity but Y313A reduces affinity by 22-fold has compelled us to modify our original model, wherein we proposed that Tyr313 interacted with salvinorin A primarily via hydrogen-bonding-type interactions. On the basis of our current findings, we propose that a hydrophobic interaction is more likely. In the proposed salvinorin A binding model, the 2-acetoxy group of salvinorin A provides the requisite hydrophobic interaction with Y313, so that salvinorin A retains affinity for the Y313F mutation but loses affinity (22-fold decrease) for the Y313A mutation.

Mutations at other residues also had significant effects on the binding of salvinorin A. Although accessible, the closest Tyr139 side-chain–ligand distance is at least 4 Å away, consistent with the weak effect of either Tyr139 mutation. In our proposed binding model, it is possible for the 17-oxo

group to form a weak hydrogen bond with Tyr139; the donor–hydrogen–acceptor (D–H–A) angle is roughly 130° when the ligand carbonyl oxygen–Tyr139 side-chain oxygen distance is 3.0 Å. However, for this hydrogen bond to be formed, the Tyr139 χ_1 torsion angle must assume values that give rise to higher energy eclipsed conformations, consistent with the modest 6-fold increase in the K_i observed for the Y139F mutation. The Y139A mutation (only 2-fold decrease in affinity) suggests that an amino acid side chain that is a small hydrophobic group, rather than a large hydrophobic group, is beneficial when the interaction takes place with a hydrophilic group on the ligand. Both mutations of Tyr320 result in the loss of affinity for salvinorin A by about 10-fold, suggesting hydrogen-bond involvement. Our proposed model interacts with Tyr320 via hydrogen bonding with the furanyl substituent of salvinorin A. However, this hydrogen bond is expected to be somewhat weaker than a normal hydrogen bond because the accepting lone-pair electrons of the oxygen atom are partially delocalized in the furan ring. The interatomic distance between the furan oxygen atom in salvinorin A and the Tyr320 side chain oxygen is 3.0 Å. Mutation of Tyr119 to either Phe or Ala decreases the affinity of salvinorin A for the KOR but to a somewhat lesser extent than for the analogous Tyr320 mutations, again indicating that hydrogen-bond interactions are involved. As with Tyr320, our proposed salvinorin A model interacts with Tyr119 via hydrogen bonding with the furanyl substituent of the ligand. It places the furan ring oxygen atom somewhat farther away from Tyr119 (3.6 Å) than from Tyr320 (3.0 Å), potentially explaining the slightly greater decrease in binding affinity for the Tyr320 mutation when compared to the analogous Tyr119 mutation.

To further explore the interactions of the salvinorins with the KOR, we employed a novel approach, whereby we combined cysteine-substitution mutagenesis with an evaluation of the binding of 2-thiosalvinorin B and salvinorin A. We reasoned that, if residues mutated to Cys were in close proximity to the thiol of 2-thiosalvinorin B, there should be an enhancement (or at least a retention) of the affinity of 2-thiosalvinorin B for the KOR, while the affinity for salvinorin A would likely decrease. An inspection of the salvinorin A binding model disclosed that Tyr313, when mutated to Cys, would yield a Cys residue that is predicted to be in close proximity to the free thiol of 2-thiosalvinorin B. In addition, mutating other nearby residues in a similar fashion would produce Cys residues nearer to other positions on the salvinorin molecule. If our proposed model is correct, mutations at these non-Tyr313 positions should affect the binding of salvinorin A and 2-thiosalvinorin B roughly equally, because salvinorin A and 2-thiosalvinorin B differ only at the 2 position. The results of these experiments are presented in Table 4 and agree with the predictions.

In our model of the KOR, the side chain of Cys315 is located in the interface between helices TM6 and TM7; therefore, it is not surprising that the mutation C315S did not result in a statistically significant change in the binding affinity for either salvinorin A or 2-thiosalvinorin B (Table 4). The most significant result from the Cys-substitution mutation studies is that the double-mutant C315S–Y313C KOR has 14.2-fold less affinity for salvinorin A than does the C315S single-mutant KOR, whereas the affinity of the double-mutant KOR for 2-thiosalvinorin B is largely unaf-

ected compared to the single-mutant C315S KOR. This would suggest that it is indeed the 2 position of the salvinorins that interact with Tyr313, because an SH-acetoxy interaction (in the case of salvinorin A) would be very weak and would increase the K_i significantly, whereas an SH-SH interaction (in the case of 2-thiosalvinorin B) would be stronger because of hydrophobic interactions and/or disulfide bond formation and would allow the double mutant to retain affinity for 2-thiosalvinorin B. We believe disulfide bond formation is unlikely because preliminary studies have demonstrated that prolonged exposure to 2-thiosalvinorin B does not lead to an irreversible loss of binding (data not shown). Our proposed model also positions the 4-methyl ester group in very close proximity to both Ile294 and Glu297. The double mutations C315S-I294C and C315S-E297C each affect both salvinorins roughly equally, increasing the affinity of both by 5–10-fold. Because both salvinorins are affected equally, it is probable that a substituent that is common to both (the 4-methyl ester group in this case, not the 2-position substituent) is interacting at Ile294 and Glu297. The nature of these interactions is unclear, because both hydrophobic and hydrophilic hydrogen-bond acceptor regions are present. However, visual inspection of space-filling models reveals that the terminal methyl of the ester group at the 4 position of salvinorin A can interact with hydrophobic portions of the Ile294 and Glu297 side chains. The lipophilic interaction between I294 and E297 and the 4 position is shown fairly clearly in Figures 5 and 6. Mutation of either of these residues to Cys would retain some hydrophobic interaction potential and perhaps more importantly would remove some of the steric bulk in the region, allowing the 4 position to more effectively associate with the side chains at positions 294 and 297. The double mutations involving Leu309 and Ser310 did not significantly alter the binding affinity of either salvinorin, and this is consistent with our proposed model complex in that these residues are not part of the ligand-binding site. No data could be obtained for the C315S-Y320C double mutation, because this mutation was inactive. 2-Thiosalvinorin B can be docked into the KOR in an orientation similar to the proposed model for salvinorin A (see Figure 6).

When these findings are taken together, they support a mode of binding whereby salvinorin A and 2-thiosalvinorin B interact with the KOR via residues that are not utilized by conventional KOR peptide and non-peptide agonists [e.g., dynorphin A (1–13) and U69593, respectively]. These residues probably line a putative binding pocket that overlaps in three-dimensional space with that used by nitrogenous KOR agonists. Thus, compounds such as U69593 are predicted to bind in approximately the same three-dimensional space but do so by utilizing different residues. It is likely that the extraordinary selectivity and potency for KORs of salvinorin A are due to the fact that it uses these “unusual” and generally nonconserved residues for ligand binding. Residues with which our proposed model interacts (namely, Ile294, Glu297, and Tyr313) are unique to the KOR. In addition, because there is no relatively strong salt bridge anchoring salvinorin A into the binding pocket and because there are many hydrogen-bonding and lipophilic interaction sites within the pocket, it would not be unexpected for the KOR to recognize salvinorin A via more than one binding mode. It is possible that these various models, taken together,

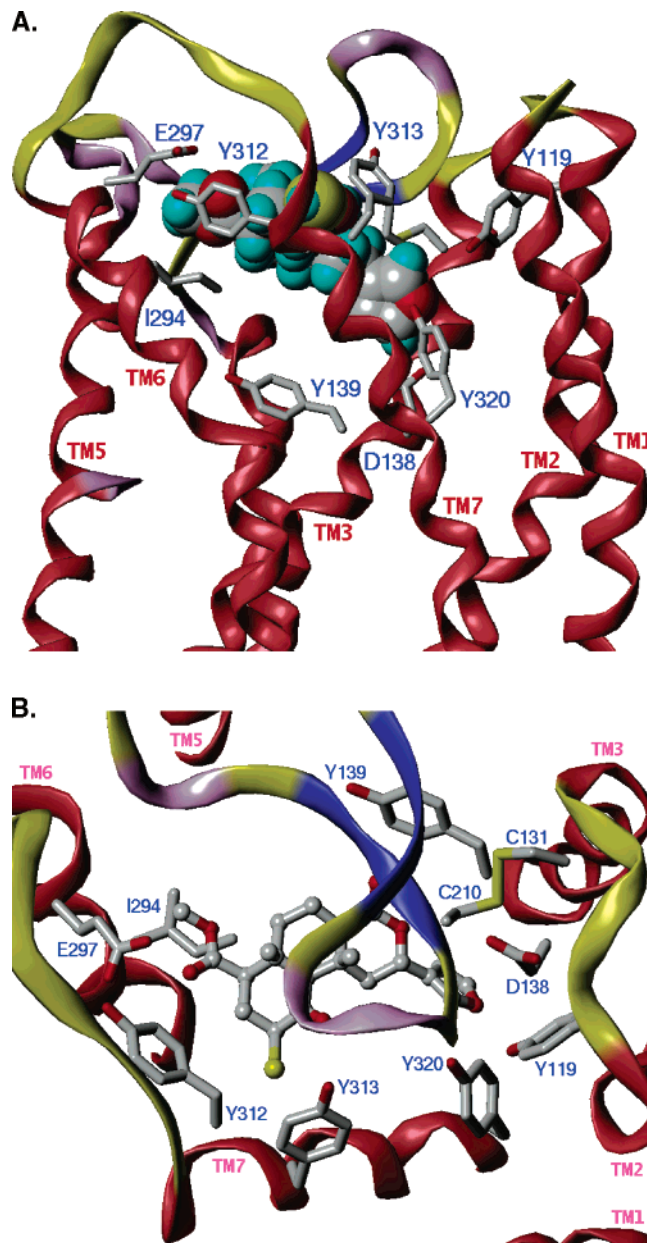


FIGURE 6: Proposed binding modes of 2-thiosalvinorin B in the KOR. (A) Proposed binding modes of 2-thiosalvinorin B in the KOR, looking through the extracellular side of the helical bundle. The KOR is color-coded based on the assignment of the secondary structure using the Kabsch-Sander (34) algorithm (red = helix, blue = β sheet, violet = turn, and yellow = coil). A view of the proposed binding model of 2-thiosalvinorin B looking from the extracellular side of the KOR beyond the e2 loop to the binding pocket.

could collectively give rise to the observed affinity and/or activation of the KOR and that no individual model would be totally responsible for the observed effects. It is likely that studies with additional salvinorin A analogues will help us to further refine the binding mode of salvinorin A and related compounds.

REFERENCES

- Valdes, L. J., Butler, W. M., Hatfield, G. M., Paul, A. G., and Koreeda, M. (1984) Divinorin A: A psychotropic terpenoid and divinorin B from the hallucinogenic Mexican mint *Salvia divinorum*, *J. Org. Chem.* 49, 4716–4720.
- Valdes, L. J., III, Diaz, J. L., and Paul, A. G. (1983) Ethnopharmacology of ska Maria Pastora (*Salvia divinorum*, Epling and Jativa-M.), *J. Ethnopharmacol.* 7, 287–312.

3. Siebert, D. J. (1994) *Salvia divinorum* and salvinorin A: New pharmacologic finding, *J. Ethnopharmacol.* **43**, 53–56.
4. Roth, B. L., Baner, K., Westkaemper, R., Siebert, D., Rice, K. C., Steinberg, S., Ernsberger, P., and Rothman, R. B. (2002) Salvinorin A: A potent naturally occurring nonnitrogenous κ opioid selective agonist, *Proc. Natl. Acad. Sci. U.S.A.* **99**, 11934–11939.
5. Sheffler, D. J., and Roth, B. L. (2003) Salvinorin A: The “magic mint” hallucinogen finds a molecular target in the κ opioid receptor, *Trends Pharmacol. Sci.* **24**, 107–109.
6. Chavkin, C., Sud, S., Jin, W., Steward, J., Zjawiony, J. K., Siebert, D., Toth, B. A., Hufeisen, S. J., and Roth, B. L. (2004) Salvinorin A, an active component of the hallucinogenic sage *Salvia divinorum*, is a highly efficacious κ opioid receptor agonist: Structural and functional considerations, *J. Pharmacol. Exp. Ther.* **308**.
7. Wang, Y., Tang, K., Inan, S., Siebert, D. J., Holzgrabe, U., Lee, D. Y., Huang, P., Li, J. G., Cowan, A., and Liu-Chen, L. Y. (2004) Comparison of pharmacological activities of three distinct κ ligands (salvinorin A, TRK-820, and 3FLB) on κ opioid receptors *in vitro* and their antipruritic and antinociceptive activities *in vivo*, *J. Pharmacol. Exp. Ther.* **308**.
8. Ballesteros, J. A., Shi, L., and Javitch, J. A. (2001) Structural mimicry in G protein-coupled receptors: Implications of the high-resolution structure of rhodopsin for structure–function analysis of rhodopsin-like receptors, *Mol. Pharmacol.* **60**, 1–19.
9. Shapiro, D. A., Kristiansen, K., Weiner, D. M., Kroeze, W. K., and Roth, B. L. (2002) Evidence for a model of agonist-induced activation of 5-HT_{2A} serotonin receptors which involves the disruption of a strong ionic interaction between helices 3 and 6, *J. Biol. Chem.* **277**, 18.
10. Shi, L., and Javitch, J. A. (2004) The second extracellular loop of the dopamine D₂ receptor lines the binding-site crevice, *Proc. Natl. Acad. Sci. U.S.A.* **101**, 440–445.
11. Shapiro, D. A., Kristiansen, K., Kroeze, W. K., and Roth, B. L. (2000) Differential modes of agonist binding to 5-hydroxytryptamine-(2A) serotonin receptors revealed by mutation and molecular modeling of conserved residues in transmembrane region 5, *Mol. Pharmacol.* **58**, 877–886.
12. Kristiansen, K. (2004) Molecular mechanisms of ligand binding, signaling, and regulation within the superfamily of G-protein-coupled receptors: Molecular modeling and mutagenesis approaches to receptor structure and function, *Pharmacol. Ther.* **103**, 21–80.
13. Stewart, D. J. Doctoral Dissertation, University of Mississippi, February 25, 2005.
14. Chavkin, C., Sud, S., Jin, W., Stewart, J., Zjawiony, J. K., Siebert, D. J., Toth, B. A., Hufeisen, S. J., and Roth, B. L. (2004) Salvinorin A, an active component of the hallucinogenic sage *Salvia divinorum* is a highly efficacious κ -opioid receptor agonist: Structural and functional considerations, *J. Pharmacol. Exp. Ther.* **308**, 1197–1203.
15. Westkaemper, R. B., and Glennon, R. A. (2002) Application of ligand SAR, receptor modeling, and receptor mutagenesis to the discovery and development of a new class of 5-HT_{2A} ligands, *Curr. Top. Med. Chem.* **2**, 575–598.
16. Baldwin, J. M., Schertler, G. F., and Unger, V. M. (1997) An α -carbon template for the transmembrane helices in the rhodopsin family of G-protein-coupled receptors, *J. Mol. Biol.* **272**, 144–164.
17. Palczewski, K., Kumasaka, T., Hori, T., Behnke, C. A., Motoshima, H., Fox, B. A., Le Trong, I., Teller, D. C., Okada, T., Stenkamp, R. E., Yamamoto, M., and Miyano, M. (2000) Crystal structure of rhodopsin: A G protein-coupled receptor [see comments], *Science* **289**, 739–745.
18. Bower, M. J., Cohen, F. E., and Dunbrack, R. L., Jr. (1997) Prediction of protein side-chain rotamers from a backbone-dependent rotamer library: A new homology modeling tool, *J. Mol. Biol.* **267**, 1268–1282.
19. Ronsisvalle, G., Pasquinucci, L., Pappalardo, M. S., Vittorio, F., Fronza, G., Romagnoli, C., Pistacchio, E., Spampinato, S., and Ferri, S. (1993) Non-peptide ligands for opioid receptors. Design of κ -specific agonists, *J. Med. Chem.* **36**, 1860–1865.
20. Lavecchia, A., Greco, G., Novellino, E., Vittorio, F., and Ronsisvalle, G. (2000) Modeling of κ -opioid receptor/agonists interactions using pharmacophore-based and docking simulations, *J. Med. Chem.* **43**, 2124–2134.
21. Mansour, A., Taylor, L. P., Fine, J. L., Thompson, R. C., Hoversten, M. T., Mosberg, H. I., Watson, S. J., and Akil, H. (1997) Key residues defining the μ -opioid receptor binding pocket: A site-directed mutagenesis study, *J. Neurochem.* **68**, 344–353.
22. Sharma, S. K., Jones, R. M., Metzger, T. G., Ferguson, D. M., and Portoghese, P. S. (2001) Transformation of a κ -opioid receptor antagonist to a κ -agonist by transfer of a guanidinium group from the 5'- to 6'-position of naltrindole, *J. Med. Chem.* **44**, 2073–2079.
23. Larson, D. L., Jones, R. M., Hjorth, S. A., Schwartz, T. W., and Portoghese, P. S. (2000) Binding of norbinaltorphimine (norBNI) congeners to wild-type and mutant μ and κ opioid receptors: Molecular recognition loci for the pharmacophore and address components of κ antagonists, *J. Med. Chem.* **43**, 1573–1576.
24. Meng, F., Hoversten, M. T., Thompson, R. C., Taylor, L., Watson, S. J., and Akil, H. (1995) A chimeric study of the molecular basis of affinity and selectivity of the κ and the δ opioid receptors. Potential role of extracellular domains, *J. Biol. Chem.* **270**, 12730–12736.
25. Watson, B., Meng, F., and Akil, H. (1996) A chimeric analysis of the opioid receptor domains critical for the binding selectivity of μ opioid ligands, *Neurobiol. Dis.* **3**, 87–96.
26. Jones, G., and Willett, P. (1995) Docking small-molecule ligands into active sites, *Curr. Opin. Biotechnol.* **6**, 652–656.
27. Jones, G., Willett, P., Glen, R. C., Leach, A. R., and Taylor, R. (1997) Development and validation of a genetic algorithm for flexible docking, *J. Mol. Biol.* **267**, 727–748.
28. Kong, H. Y., Raynor, K., and Reisine, T. (1994) Amino acids in the cloned κ receptor that are necessary for the high affinity agonist binding but not antagonist binding, *Regul. Pept.* **54**, 155–156.
29. Ott, D., Frischknecht, R., and Pluckthun, A. (2004) Construction and characterization of a κ opioid receptor devoid of all free cysteines, *Protein Eng. Des. Sel.* **17**, 37–48.
30. Xu, W., Li, J., Chen, C., Huang, P., Weinstein, H., Javitch, J. A., Shi, L., de Riel, J. K., and Liu-Chen, L. Y. (2001) Comparison of the amino acid residues in the sixth transmembrane domains accessible in the binding-site crevices of μ , δ , and κ opioid receptors, *Biochemistry* **40**, 8018–8029.
31. Bourne, H. R., and Meng, E. C. (2000) Structure. Rhodopsin sees the light, *Science* **289**, 733–734.
32. Fowler, C. B., Pogozeva, I. D., LeVine, H., III, and Mosberg, H. I. (2004) Refinement of a homology model of the μ -opioid receptor using distance constraints from intrinsic and engineered zinc-binding sites, *Biochemistry* **43**, 8700–8710.
33. Pogozeva, I. D., Lomize, A. L., and Mosberg, H. I. (1998) Opioid receptor three-dimensional structures from distance geometry calculations with hydrogen bonding constraints, *Biophys. J.* **75**, 612–634.
34. Kabsch, W., and Sander, C. (1983) Dictionary of protein secondary structure: Pattern recognition of hydrogen-bonded and geometrical features, *Biopolymers* **22**, 2577–2637.

BI050490D